Catalysis Today 180 (2012) 34–41

Contents lists available at ScienceDirect

Catalysis Today

journal homepage: www.elsevier.com/locate/cattod

Cooperative effect between copper and gold on ceria for CO-PROX reaction

Juliana da Silva Lima Fonseca[a,b], Hadma Sousa Ferreira[a,b], Nicolas Bion[a], Laurence Pirault-Roy[a], Maria do Carmo Rangel[b], Daniel Duprez[a], Florence Epron[a,*]

[a] LACCO, Laboratoire de Catalyse en Chimie Organique, Université de Poitiers & CNRS, 40, Av. Recteur Pineau, 86022 Poitiers Cedex, France
[b] GECCAT Grupo de Estudos em Cinética e Catálise. Instituto de Química, Universidade Federal da Bahia. Campus Universitário de Ondina, Federação, 40 170-280, Salvador, Bahia, Brazil

ARTICLE INFO

Article history:
Received 31 January 2011
Received in revised form 18 May 2011
Accepted 5 June 2011
Available online 2 July 2011

Keywords:
PROX preferential oxidation of CO
Gold–copper–ceria catalysts
Gold–copper interactions

ABSTRACT

1.1 wt% Cu and 1 wt% Au/CeO_2 catalysts were prepared by impregnation of a high-surface area ceria (>200 $m^2\,g^{-1}$) with copper nitrate and dimethyl(acetylacetonate) gold(III), respectively. They were dried and calcined in air at 300 °C. They were denoted Au/CeO_2 and CuO_x/CeO_2. The same procedure was used to prepare a composite catalyst by impregnation of gold on the CuO_x/CeO_2 catalyst (Au-CuO_x/CeO_2). XRD reveals that ceria is poorly crystallized (crystallite particle size of 11.4 nm) while Au and CuO_x cannot be detected. Redox properties were evaluated by temperature-programmed reduction (TPR) and oxygen storage capacity (OSC) measurements. While gold is easily reduced below 100 °C, copper oxide reduces to Cu^0 at 266 °C. Copper and gold promote the surface reduction of ceria. OSC measurements confirm that about one monolayer of ceria can be reduced at 400 °C. The performances of the catalysts in PROX reaction (2%CO + 2%O_2 + 70%H_2 in He) were measured between room temperature and 300 °C. At low temperature (below 120 °C), there is an increase in CO conversion up to 100%. Au/CeO_2 is about 9 times more active than CuO/CeO_2 but it is much less selective (50–60% of selectivity for Au instead of 100% for CuO_x). Au-CuO_x/CeO_2 exhibits an intermediary behavior with both good activity and good selectivity. A decrease in CO conversion is observed above 120 °C for all the catalysts. It is due to the reverse water gas shift reaction (RWGS) tending to reform CO from CO_2 and H_2. This behavior is more marked for Au than for CuO_x and Au-CuO_x catalysts, which shows that gold is very active in RWGS. The three catalysts are deactivated by CO_2 while only copper is very sensitive to steam. An interesting cooperative effect is shown for the Au-CuO_x/CeO_2 catalyst: (i) moderate and totally reversible inhibition by CO_2 and (ii) absence of inhibition by steam.

1. Introduction

In recent times, the concern for environment protection and for the efficient use of energy has increased the interest for new technologies, especially for fuel cell, the most promising source of energy generation in this century. Hydrogen, a clean fuel that emits no pollutant when burned, is considered as the main source of energy for the future and the most suitable for fuel cells [1]. Proton exchange membrane fuel cell (PEMFC) is by far the most advanced type for various applications, both mobile and stationary, especially for electronic devices, due to their special characteristics of high energy conversion efficiency at low operating temperature (<100 °C), rapid start-up and fast response to load variations [2]. For practical purposes, hydrogen has to be produced on board and then a reformer and units for removal of carbon monoxide should be provided in the fuel processor for PEMFCs [3]. In this case, hydrogen can be produced from liquid fuels or hydrocarbons through steam reforming, partial oxidation or autothermal reforming, followed by water gas shift reaction (WGSR) [4]. However, the small amount of carbon monoxide remaining in the stream (about 1% by volume) can poison the anodic platinum-electrocatalyst thus requiring its removal [5]. Among the different techniques used for hydrogen purification, the preferential oxidation of carbon monoxide (PROX) is the most simple, efficient and economical way to reduce the concentration of carbon monoxide to a level of 10 ppm [4].

The preferential oxidation of carbon monoxide (Eq. (1)) involves the oxidation of carbon monoxide, in a reformate stream, to carbon dioxide on a suitable catalyst using molecular oxygen [6,7]. Other reactions (Eqs. (2–5)) can occur, due to the high concentration of hydrogen in the feed gas and should be avoided because of hydrogen consumption.

$$CO + \tfrac{1}{2}O_2 \rightarrow CO_2 \quad (1)$$

* Corresponding author. Tel.: +335 49 45 48 32; fax: +335 49 45 37 41.
E-mail address: florence.epron.cognet@univ-poitiers.fr (F. Epron).

0920-5861/$ – see front matter © 2011 Elsevier B.V. All rights reserved.
doi:10.1016/j.cattod.2011.06.008

$$H_2 + ½O_2 \rightarrow H_2O \quad (2)$$

$$H_2 + CO_2 \leftrightarrows H_2O + CO \quad (3)$$

$$3H_2 + CO \leftrightarrows H_2O + CH_4 \quad (4)$$

$$4H_2 + CO_2 \leftrightarrows CH_4 + 2H_2O \quad (5)$$

$$2CO \leftrightarrows C + CO_2 \quad (6)$$

Several studies have been addressed to find a suitable catalyst for this system. The main challenges are related to high activity at low temperatures and high selectivity for carbon monoxide oxidation, avoiding the undesirable oxidation of hydrogen which would decrease the overall efficiency of the process. In addition, it should be able to operate in a relatively wide temperature range to achieve conversions of carbon monoxide above 99%, since the PROX unit is disposed between the reactor of WGSR at low temperature (200 °C) and the PEMFC (about 80 °C). Also, the catalyst should be stable and highly resistant against deactivation by water and carbon dioxide from the feed [8,9]. Moreover, a careful control of oxygen to carbon dioxide ratio as well as of temperature is needed, since the excess oxygen can also oxidize the hydrogen in the feed. Overall, the performance of PROX catalysts depends on the kind of the catalyst, O_2/CO ratio, contact time and reactor design [9].

Metallic gold and copper oxides are known to be active catalysts for CO oxidation, most studies showing that Au is more active than CuO_x [10]. This ranking of activity is generally observed on ceria-supported catalysts for reactions at moderate temperatures [11]. The reverse order has been reported for CO oxidation at 300 °C probably because CuO_x catalysts are more stable than gold ones [12,13]. Ceria is a remarkable support both for Au and CuO_x as well as for many other oxides because it is able to maintain a high dispersion of metal and oxides [14–16] and to favor oxygen transfer from metal to support and vice versa [17].

Activity of gold and copper for H_2 oxidation in gas phase is less documented. While oxygen titration of chemisorbed hydrogen is currently carried out at room temperature to characterize noble metal catalysts (Pt, Rh,...) [18–21], this technique cannot be applied to gold and copper because hydrogen cannot generally chemisorb on these metals [22] even though some possibilities might exist on very small clusters of gold [23]. This is due to the very low heat of adsorption of H_2 on Au and Cu, below 40 kJ mol^{-1} [24]. However, much information is available on the reduction of oxygen by hydrogen in liquid phase (PEM fuel cells) [25]. Oxygen evolution in the course of the reaction may lead to different mechanisms of H_2 oxidation. On some metals, O_2 dissociation prevails (Ni, Cu,...) while, on other metals, associative mechanisms leading to peroxyl or peroxide intermediates can be observed (Pt, Pd, Ag,...). H_2 oxidation over gold could produce large amounts of hydrogen peroxide, which means that a two-electron process is favored on this metal. This particular behavior of gold (alone or in association with palladium) explains why it may be used for direct H_2O_2 synthesis from H_2–O_2 mixtures [26]. In these previous papers, only the behavior of gold and copper in the metallic form are taken into consideration. Activity of CuO_x for H_2 oxidation is rarely reported. Nevertheless, Potemkin et al. reported that CuO_x-CeO_2 catalysts in which some Cu^0 species could be detected were significantly less selective in PROX reaction [27]. This tends to prove that metallic copper is much more active for H_2 oxidation than copper oxides.

Noble metal-based catalysts have been the most studied ones for PROX reaction, especially those based on platinum and ruthenium [6,28,29]. They have shown high intrinsic activity but low availability of surface oxygen [30], which is overcome by the use of reducible supports, which provide oxygen for the reaction and significantly increase the performance of these systems [28]. Nevertheless, the strong adsorption of carbon monoxide on the metal limits the access of other molecules, including oxygen, decreasing the rate of re-oxidation by molecular oxygen on the surface and thus reducing the overall rate of carbon monoxide oxidation [31]. Moreover, the overall selectivity of PROX is decreased due to insufficient coverage of the catalyst surface and the consequent occurrence of hydrogen oxidation [32]. On the other hand, catalysts based on gold supported on reducible oxides such as cerium oxide [33], iron oxide [34] or titanium oxide [35] have shown higher activity than those based on platinum, but were not tolerant to water or carbon dioxide [34]. A completely different mechanism occurs over these catalysts as compared to platinum-based systems due to high activity of gold for carbon monoxide oxidation, even at room temperature [36]. In fact, the adsorption of carbon monoxide on gold is weaker than for platinum [30], but gold activates carbon monoxide oxidation at lower temperatures at higher rates than hydrogen oxidation. Thus, gold can be considered as an intrinsic catalyst for this reaction, since it activates the desired species of oxygen, increasing more the rate of carbon monoxide oxidation than hydrogen oxidation. Moreover, oxygen has a low adsorption coefficient on gold and then the use of active supports, such as iron oxide, titanium oxide or cerium oxide, increases the rate of carbon monoxide oxidation by providing adsorption sites for oxygen, thus supplying it during the reaction [32]. Despite some advantages, the high cost and limited availability of noble metals, as well as their sensitivity to poisoning by sulfur, water and carbon dioxide, have motivated research into other alternatives such as non-noble metal oxides [5,31].

Currently, the most studied catalysts for PROX reaction, as alternative to noble metals, are those based on metal oxides, particularly copper oxide due to its high activity and selectivity in carbon monoxide oxidation [37]. In particular, the catalysts based on copper and cerium (CuO-CeO_2) have been proposed as candidates for the PROX reaction [38,39]. They are more active and remarkably more selective than the noble metals and are active at significantly lower temperatures (100–200 °C) than the platinum catalysts. They are also very stable under the reaction conditions and can tolerate high concentrations of carbon dioxide and water, besides the low cost. Moreover, they do not promote the reverse water gas shift reaction in the temperature range of PROX reaction. Compared to the catalysts of platinum group, they present higher activity and selectivity and compared to gold catalysts, they are less active but more selective and more stable [40].

The high performance of such systems in PROX reaction has been assigned to the synergistic redox properties, involving reduction and oxidation of copper and cerium arising from the sites in the interface copper oxide-cerium oxide [41]. Thus, the active sites are related to well dispersed states of copper, probably as clusters in strong interaction with ceria [42]. It was proposed [43] that the well dispersed copper oxide on cerium oxide, which is more reducible at lower temperatures than bulk copper oxide, can adsorb carbon monoxide more efficiently. Moreover, copper increases the redox properties, the ability of oxygen storage and the thermal stability of ceria [44,45]. As a result, this catalyst exhibits high activity and selectivity for carbon monoxide oxidation at low temperatures [46].

Despite the binary CuO-CeO_2 catalysts present high performance in the PROX process, it is known [46,47] that these systems go on gradual deactivation during the PROX reaction, which limits its use under practical conditions. However, few studies have focused on the causes of deactivation [48,49]. These studies suggest that the coke deposition is not relevant, but the accumulation of hydroxy species on the interfacial sites and sintering of copper are the factors determining the stability of these systems [49].

In the present work, the cooperative effect between copper and gold on ceria was studied aiming to find efficient catalyst for PROX reaction, by combining the properties of these two metals.

2. Experimental

2.1. Catalysts preparation

The CuO_x/CeO_2 catalyst was prepared by simple impregnation of the support (CeO_2, Rhodia) with the corresponding aqueous solution of $Cu(NO_3)_2{\cdot}3H_2O$ (Prolabo, ≥99.0%). The aqueous solution was mixed with the support under stirring for 12 h and the catalyst was subsequently dried at 60 °C, for 6 h, and at 120 °C, overnight, and finally calcined for 4 h at 450 °C under flowing air (30 mL min^{-1}).

The gold catalyst $Au/CeO_2$was prepared by impregnation in organic medium under argon atmosphere. The gold precursor was dimethyl(acetylacetonate)gold(III) [$Au(acac)_3$] supplied by Strem Chemical. Before the impregnation, 0.5 g of the support was pretreated under flowing Ar (60 mL min^{-1}), at 400 °C for 2 h, heating rate 2 °C min^{-1}, and cooled down to room temperature. It was first immersed in 10 ml toluene, then 10 ml toluene solution of $Au(acac)_3$ was added, and kept for 6 h at 40 °C in bubbling Ar. The amount of $Au(acac)_3$ dissolved in toluene corresponded to 1 wt% of gold. Toluene was drained from the sample that was dried under argon flow during 15 h, at 40 °C. The samples were calcined for 1 h at 300 °C, 2 °C min^{-1}, under flowing air (30 mL min^{-1}). The same procedure was employed to prepare a bimetallic Au-CuO_x/CeO_2 catalyst, using the CuO_x/CeO_2 instead of CeO_2 to deposit gold.

The bulk chemical composition is measured by ICP-OES using a Perkin Elmer Optima 2000 DV. The samples were mineralized with a mixture of nitric and chloride acids and the results of this analysis are showed in Table 1.

2.2. Specific surface measurement

The specific surface area and porosity measurements were carried out by nitrogen adsorption at −196 °C, in a Micromeritics equipment, model TRISTAR 3000. The specific surface areas were calculated using the BET (Brunauer–Emmett–Teller) model. For the analysis, about 0.2 g of the sample were heated up to 250 °C under vacuum in order to eliminate the adsorbed species.

2.3. X-ray diffraction

X-ray diffraction measurements were performed at room temperature in a Bruker AXS D5005 X-ray diffractometer, working with CuKα radiation (λ = 1.54184 Å), generated at 40 kV and 40 mA. Signal is recorded for 2θ between 20° and 80° with a step of 0.025° (step time: 1 s). Phase identification is made by comparison with JCPDS database No. 065-2975, for the cerium oxide and No. 078-0428, for the copper oxide.

2.4. Temperature programmed reduction (TPR)

Prior to the TPR test, the catalyst (100 mg) was first pretreated *in situ* under oxygen at 300 °C for 30 min and cooled down to room temperature. After flushing under argon for 15 min, the reduction was carried out from room temperature up to 600 °C under a 1% H_2/Ar mixture, using a 2 °C min^{-1} as heating rate. The measurements of the hydrogen consumption were made by a AutoChem II/Micromeritics apparatus, using a thermal conductivity detector.

2.5. Oxygen storage capacity (OSC)

OSC measurements were carried out in an atmospheric glass fixed bed reactor placed in an electrical oven connected to a Porapak column and a TCD. The sample (6–8 mg) was placed into the reactor and heated up to 400 °C under a continuous flow of helium (30 mL min^{-1}) at atmospheric pressure. At this temperature, 10 pulses (0.265 mL) of pure O_2 were introduced to oxidize completely the sample and a He flow was passed through the sample for 10 min to purge it. Then, 10 pure CO pulses were injected before a new purging step of 10 min with He. The oxygen storage capacity (OSC) was calculated from the first CO pulse. Then, the oxygen storage complete capacity (OSCC) value was evaluated from the total amount of CO consumed at the end of the CO pulse series. The OSCC value corresponds to the total amount of reactive oxygen.

2.6. Catalyst tests

Catalytic tests were carried out in a conventional glass fixed-bed reactor placed in an electrical oven. Because of the small size of the catalyst bed, it was assumed that there was no significant temperature profile in the system. The standard reaction mixture consisted in 2 vol.% CO, 2 vol.% O_2, 70 vol.% H_2, and He as a balance (standard gas mixture), and the total inlet gas flow rate was fixed at 100 mL min^{-1}. All gases used were analytical grade (Alphagas-1) and were supplied by Air Liquide. Before each experiment the catalyst was pre-conditioned *in situ* under 30 mL min^{-1} of flowing 20 vol.% O_2/He, heating rate 2 °C min^{-1}, at 300 °C for 30 min and then 10 min under He flow to purge the sample.

In the experiments carried out by decreasing the temperature, three analysis of the gas at the reactor outlet were made at the same temperature, every 20 °C, with an interval of 4 min between each injection. Similar activity and selectivity values were obtained. In these experiments, the mass of catalyst was fixed at 100 mg.

In the isothermal experiments at 100 °C, catalysts were submitted to the same pretreatment. After purging with He, the standard gas mixture was passed through the system for 15 min before starting the cooling down. After 15 min at stabilized temperature (100 °C), the first injection was made. In the first step, reaction was carried out for 5 h, with the same composition of the standard gas mixture, and injections were made every 15 min. After this time, 10vol.% CO_2 was added to the feed and the reaction was performed for 1 h more (4 injections). Then, the standard gas mixture was again passed through the catalyst (2 injections) and finally 2 vol.% of H_2O were added to the standard feed, doing 4 injections (1 h). The mass of catalyst was fixed at 10 mg (for Au/CeO_2 and Au-CuO_x/CeO_2) and 20 mg (for CuO_x/CeO_2). All the catalysts were diluted in α-Al_2O_3 to obtain a total mass of 100 mg.

The gases were separated by a gas chromatograph (Varian 3900) equipped with a Altech® CTR I column capable of separating H_2, O_2, CO_2, N_2, CH_4 and CO. Helium was used as the carrier gas. The oxygen and the carbon monoxide conversions were based on the oxygen and the carbon monoxide consumption, respectively:

$$X_{O_2} = \frac{F_{O_2}^{in} - F_{O_2}^{out}}{F_{O_2}^{in}} \times 100$$

$$X_{CO} = \frac{F_{CO}^{in} - F_{CO}^{out}}{F_{CO}^{in}} \times 100$$

where X is percentage of conversion and F is the (inlet or outlet) molar flow of the indicated gas. The selectivity is calculated by:

$$S_{CO_2} = \frac{F_{CO}^{in} - F_{CO}^{out}}{2 \times (F_{O_2}^{in} - F_{O_2}^{out})} \times 100$$

It represents the percentage of O_2 having reacted with CO. Carbon monoxide is exclusively converted to CO_2. Methanation reactions do not occur.

Table 1
Textural, chemical parameters and H_2 consumption measured in the temperature-programmed reduction (TPR) of CeO_2, CuO_x/CeO_2, Au/CeO_2 and $Au\text{-}CuO_x/CeO_2$ catalysts.

Samples	S_{BET} ($m^2\,g^{-1}$)	Au content (wt%)	Cu content (wt%)	Total H_2 consumption ($\mu mol\,g^{-1}$)	H_2 consumption by support reduction[a] ($\mu mol\,m^{-2}$)	N_L[b]
CeO_2	222			537	2.4	0.45
CuO_x/CeO_2	212		1.10	1421	6.0	1.10
Au/CeO_2	232	0.98		1009	4.0	0.74
$Au\text{-}CuO_x/CeO_2$	210	1.00	1.10	903	3.2	0.59

[a] Obtained considering the metal completely oxidized at the beginning of the TPR and removing the H_2 consumed by reduction of $CuO \rightarrow Cu^0$ and $Au_2O_3 \rightarrow Au^0$.
[b] N_L: number of oxygen layers of ceria involved in the TPR when 425 °C is reached.

3. Results

3.1. Characterization

After calcination at 450 °C, the specific surface area of ceria is of 222 $m^2\,g^{-1}$. The samples containing copper exhibit slightly lower surfaces whereas the BET surface of the Au/CeO_2 sample surprisingly increased (Table 1). Taking into account the percentage of error in the measurement we could consider all the specific surfaces quite similar. The structural characterization by powder X-ray diffraction was performed for each sample (Fig. 1). In all the patterns, only the peaks characteristic of the face-centered cubic fluorite-type typical of CeO_2 were observed. No peak corresponding to copper or gold species were discernable in the patterns. When low contents of metal are added like in the current case, it becomes always difficult to conclude if the absence of signal is due either to the size of the crystallites, which are too small, or to the limit of detection of the instrument. An average ceria crystallite size of 11.4 nm, calculated from the Debye–Scherrer equation using the peaks corresponding to 111, 200, 220 and 311 planes, was maintained after addition of copper and/or gold. This crystallite size of ceria is higher than the size calculated from the BET area supposing spherical particles of a fully crystallized material (4–5 nm). This means that the ceria (222 $m^2\,g^{-1}$) is partly amorphous and/or contains very small crystallites not easily detectable by XRD.

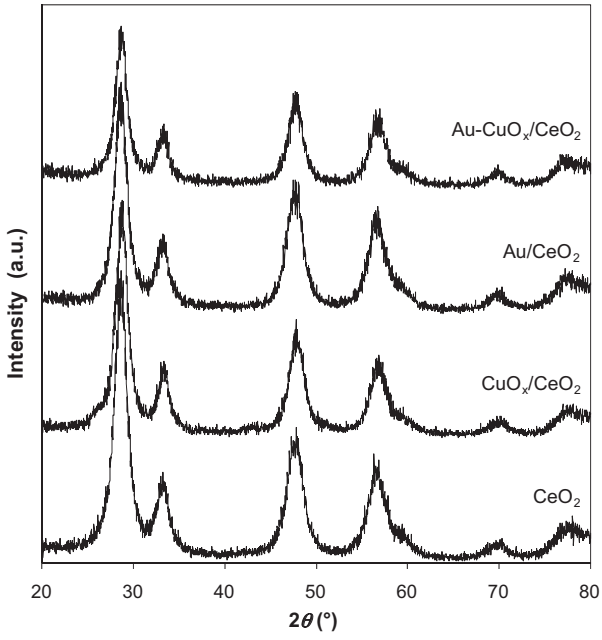

Fig. 1. Powder X-ray diffraction patterns of CeO_2, CuO_x/CeO_2, Au/CeO_2 and $Au\text{-}CuO_x/CeO_2$ catalysts.

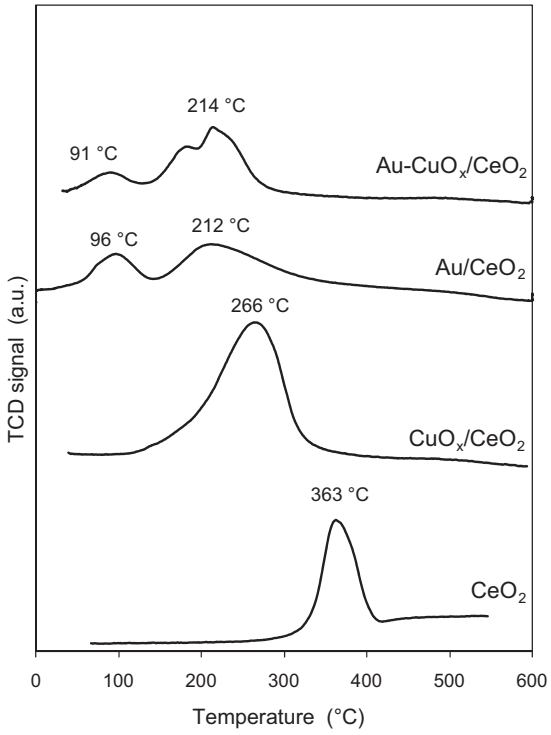

Fig. 2. Temperature-programmed reduction profiles of CeO_2, CuO_x/CeO_2, Au/CeO_2 and $Au\text{-}CuO_x/CeO_2$ catalysts.

3.1.1. Temperature-programmed reduction

While noble metals significantly enhance the oxygen storage capacity of ceria [45,50–54], the effect of copper [39,45,55] and gold [55–57] on the redox properties of ceria are less pronounced. However, both copper and gold can promote the reduction of Ce^{4+} to Ce^{3+} ions, at least in the vicinity of CuO_x or Au species and probably on a large fraction of the ceria surface.

The profiles of the temperature-programmed reduction (TPR) performed on each sample are shown in Fig. 2 where the TCD signal is proportional to the amount of H_2 consumed. We also reported in Table 1 the values of H_2 consumption after integration of the profiles between 30 and 425 °C. In the range 30–600 °C, ceria exhibits one intense peak centered at 363 °C, which matches with the reduction of the oxide surface. The behavior of the ceria has been largely studied using H_2-TPR [50] and it is clearly established that two main peaks are generated in such an experiment: the former corresponds to the reduction of the surface oxygen layer of ceria around 400 °C whereas the latter is due to the reduction of the bulk and occurs when the temperature reaches 800 °C. Other authors [58] already reported the beneficial effect of copper on the reduction of the ceria surface. In Fig 2, we noticed, in the profile of the $CuO_x/CeO2$ sample, a shift of the peak assigned to the reduction of the ceria surface from 363 to 266 °C. This result is due to a promotion of the ceria surface by the presence of copper. It is worth noting that only one wide peak

is present in the range of temperature recorded. We suggest that the total consumption of H_2 characterized by this peak includes the H_2 consumed by CuO reduction as well as the H_2 consumption due to the reduction of the ceria surface. The consumption of H_2 started at 125 °C and showed that ceria also promoted the reduction of CuO, which is usually expected for unsupported CuO around 250 °C. Such inter-promotion in CuO_x/CeO_2 mixed oxide resulting from copper-cerium interaction was already described [39]. If we consider that CuO is reduced into Cu^0, we are able to remove the contribution of copper from the total amount of H_2 consumed. The rest should represent the amount of hydrogen involved in the reduction of the ceria. One can see that the addition of copper enabled the reduction of 2.5 times more oxygen atoms of the ceria surface (6 μmol O m^{-2} for CuO_x/CeO_2 against 2.4 μmol O m^{-2} for CeO_2). Using the same argument than in the work detailed by Madier et al. [59], we reported, in Table 1, the number of oxygen layers of ceria, N_L, involved in the TPR. This number is 1 when 5.4 μmol O m^{-2} are removed from the surface. This value also represents the theoretical OSC that will be discussed later. In the case of bare ceria, less than 50% of the first layer of oxygen is reduced at 425 °C. The addition of copper allows obtaining the whole reduction of the surface at the same temperature.

The profile of the gold-promoted ceria (Au/CeO_2) catalyst consists in a low temperature peak with a maximum at 96 °C and a second one, broader, centered at 212 °C. As mentioned in other publications [55,60] the first peak could be assigned to the reduction of oxygen species on the small gold particles whereas the second one would be connected with the surface ceria reduction. If the oxidation state of gold species is often a controversial subject when they are supported on cerium oxide, it is reasonable to suppose them oxidized after calcination of the solid at 300 °C. However, the integration of the first peak displays an amount of H_2 consumed that cannot be explained only by the reduction of the metal, even assuming a total reduction of Au_2O_3 into Au^0. We speculated that a part of the ceria surface located at the interface with some gold particles was reduced at very low temperature, the rest being reduced in a wide range of temperatures (the peak at 212 °C displayed a long and flat tail at higher temperatures). The total amount of H_2 consumed at 425 °C showed that only 75% of the first layer of oxygen were removed that was inferior to the value calculated in CuO/CeO_2. The result obtained for the bimetallic $Au\text{-}CuO_x/CeO_2$ was quite surprising since the reducibility of the ceria in this solid is lower than in the case of the monometallic samples. It may be explained by a different initial oxidation state of gold and/or copper in the bimetallic catalyst compared to that in the monometallic ones.

3.1.2. Oxygen storage capacity

OSC and OSCC were measured at 400 °C on the four catalysts and the values obtained were reported in Table 2. We expressed the storage capacities in μmol O per g or per m^2, which corresponds to the amount of oxygen removed by reduction with CO to produce CO_2. We can discuss the data in comparison with the results of TPR we commented previously. In the case of ceria, both values of OSC (calculated on the first CO pulse) and OSCC (calculated on the 10 first pulses) were low and showed that the process was limited to less than 20% of the ceria surface. This percentage, inferior to the percentage obtained by TPR, indicated that the reduction under H_2 in a plug-flow reactor was more efficient than that with a CO multi-pulse treatment.

The real OSC values Au/CeO_2, CuO_x/CeO_2 and $Au\text{-}CuO_x/CeO_2$, reported in Table 2, were obtained considering that the metal was completely oxidized after oxidizing pre-treatment and completely reduced after the first CO pulse. According to this hypothesis we subtracted from the total OSC value the amount of oxygen that could come from the metal (157 μmol O g^{-1} for CuO_x, 75 μmol O g^{-1} for Au_2O_3, and 232 μmol O g^{-1} for the bimetallic catalyst) to obtain the real OSC and OSCC values due to the ceria. The measurements on these solids showed that the addition of gold and copper does not change the reducibility of ceria during OSC experiment, since the real OSCC value, and consequently the number of oxygen layers of ceria involved in the OSCC process, is similar whatever the catalyst.

3.2. Activity and selectivity of the ceria-supported catalysts

First of all, the catalysts were evaluated in standard gas mixture conditions, i.e. without CO_2 and H_2O in the gas phase, in a wide range of temperature, starting from 300 °C and decreasing the temperature to room temperature by steps of 20 °C. Three measurements were performed at each temperature. Fig. 3(a) and (b) show the evolution of the CO conversion and selectivity in CO_2, respectively, as a function of temperature in the 10–300 °C range for the 3 catalysts. At first, it can be seen from Fig. 3(a) that at low temperature, lower than 100 °C, the monometallic Au/CeO_2 is the most active catalyst with 50% of CO converted at 40 °C, whereas to obtain such a conversion with CuO_x/CeO_2, a temperature higher than 80 °C is needed. A similar trend was observed by Avgouropoulos et al. [61] on their Au/Ceria and CuO/Ceria catalysts. The $Au\text{-}CuO_x/CeO_2$ has an intermediate behavior. The maximum of CO conversion is reached at 80 °C for the Au/CeO_2 catalyst, with 98% of CO converted, a similar conversion being obtained with $Au\text{-}CuO_x/CeO_2$. A temperature as high as 120 °C is needed to reach a complete conversion of CO over CuO/CeO_2. When the temperature increases, the conversion of CO decreases progressively in the presence of the Au/CeO_2 catalyst, whereas it remains stable, at 100% up to 180 °C, for the two others. This can be explained by a weaker CO binding on Au than on copper. It has been demonstrated by periodic density functional

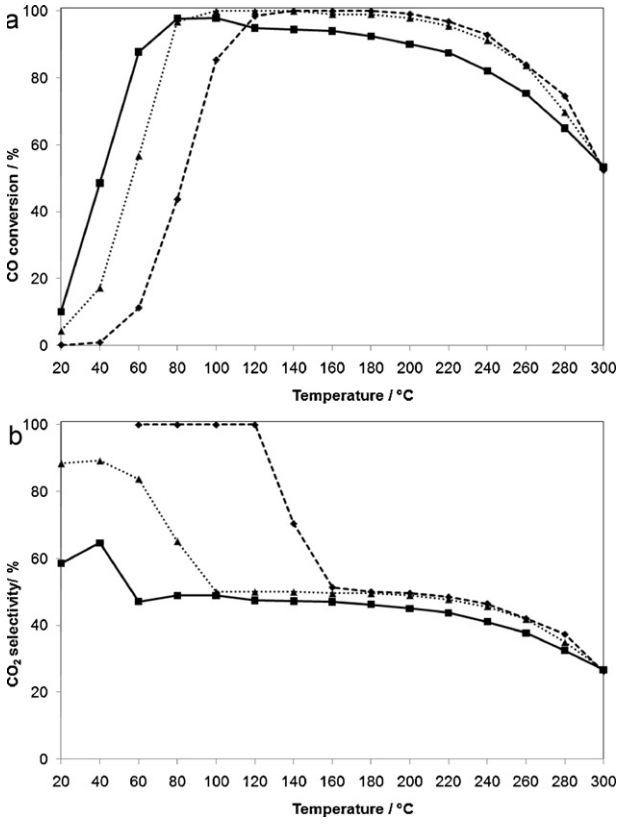

Fig. 3. Evolution of CO conversion (a) and selectivity in CO_2 (b) versus temperature obtained during the CO-PROX over Au/CeO_2 (■), CuO_x/CeO_2 (♦) and $Au\text{-}CuO_x/CeO_2$ (▲). Experimental conditions: 2% CO, 2% O_2, 70% H_2, 26% He, 100 mg of catalyst, total gas inlet: 100 mL min^{-1}.

Table 2
Oxygen Storage Capacities of CeO_2, CuO_x/CeO_2, Au/CeO_2 and $Au\text{-}CuO_x/CeO_2$ catalysts at 400 °C.

Samples	OSC and OSCC (μmol O g^{-1})				OSCC (μmol O m^{-2})	N_L [c]
	Total OSC[a]	Real OSC[b]	Total OSCC[a]	Real OSCC[b]		
CeO_2	133	133	240	240	1.08	0.19
CuO_x/CeO_2	411	254	434	277	1.31	0.23
Au/CeO_2	225	149	316	241	1.04	0.18
$Au\text{-}CuO_x/CeO_2$	459	225	468	236	1.12	0.20

[a] Total OSC and OSCC values are based on the amount of CO_2 produced by the reduction of the catalyst with the first (OSC) and the 10 first (OSCC) pulses of CO.
[b] Real OSC and OSCC values are obtained in considering the metal completely oxidized (CuO or Au_2O_3) before the first CO pulse and removing from total OSC and OSCC values the contribution due to the reduction of the metal.
[c] N_L: number of oxygen layers of ceria involved in the OSCC process.

theory (DFT) calculations and micro-kinetic modeling [62] that the ratio $\theta CO/\theta H$ decreases significantly on gold, more than on copper, as temperature increases. After 180 °C, an important decrease in the conversion is observed for all the catalysts. As the test is performed by decreasing the temperature, the lower CO conversion at high temperature cannot be due to the deactivation of the catalyst and is more likely to be linked to the reverse water gas shift reaction, which is thermodynamically favored. Interestingly, these results show that, for the conversion of CO, the $Au\text{-}CuO_x/CeO_2$ catalyst benefits from the advantage of each active phase: it is able to completely convert CO at low temperature as the Au/CeO_2 catalyst, whereas, when the temperature increases, his behavior is similar to that of the CuO_x/CeO_2 catalyst, with a complete conversion in a wide range of temperature.

As far as the selectivity in CO_2 (Fig. 3(b)) is concerned, one can see that at low temperature, the Au/CeO_2 is by far the less selective catalyst, whereas, the CuO_x/CeO_2 catalyst is the only catalyst able to selectively convert all the CO into CO_2, i.e. without oxidation of hydrogen, even at 100% of CO conversion, in accordance with the results of Avgouropoulos et al. [61]. The presence of gold and copper together, in the $Au\text{-}CuO_x/CeO_2$ catalyst, allows one to increase the selectivity compared to Au/CeO_2: at 80 °C, the selectivity is of 65% and 50% for $Au\text{-}CuO/CeO_2$ and Au/CeO_2, respectively, for the same CO conversion (98%). At temperatures higher than 160 °C, the selectivity of the three catalysts can be considered as similar.

To conclude this part, the $Au\text{-}CuO_x/CeO_2$ catalyst is more active in CO conversion than the CuO_x/CeO_2 one at low temperature but presents a similar behavior at temperature higher than 120 °C. Its selectivity into CO_2 is intermediate between those of Au/CeO_2 and CuO_x/CeO_2. At 100 °C, the activity in CO conversion decreases in the following order: $Au\text{-}CuO_x/CeO_2 > Au/CeO_2 \gg CuO_x/CeO_2$ with CO conversion of 100%, 98% and 85%, respectively.

3.3. Stability of the catalysts

The stability of the three catalysts was evaluated at 100 °C during 8 h. CO_2 and H_2O were alternatively introduced in the gas feed after 5 and 6h 30 of time on stream, respectively, in order to evaluate the catalytic performances in more realistic reaction conditions. Results of CO conversion and selectivity in CO_2 are reported in Fig. 4 (a) and (b), respectively. Fig. 4(a) shows that, even if the mass of catalyst is lower than the one used in the previous paragraph, the activity ranking is similar, the $Au\text{-}CuO_x/CeO_2$ being the most active catalyst. When CO_2 is added, an important deactivation is observed whatever the catalyst, although the CuO_x/CeO_2 catalyst seems to be less affected. This deactivation can be explained by a competitive adsorption of CO_2 on the gold or copper surface or at the interface with the support and to an increase formation of deactivating carbonates [34]. When CO_2 is removed from the gas phase, the initial CO conversion is nearly completely recovered, except for the Au/CeO_2 sample, which is only partially reactivated. CO_2 is likely to be more strongly adsorbed on this type of catalyst.

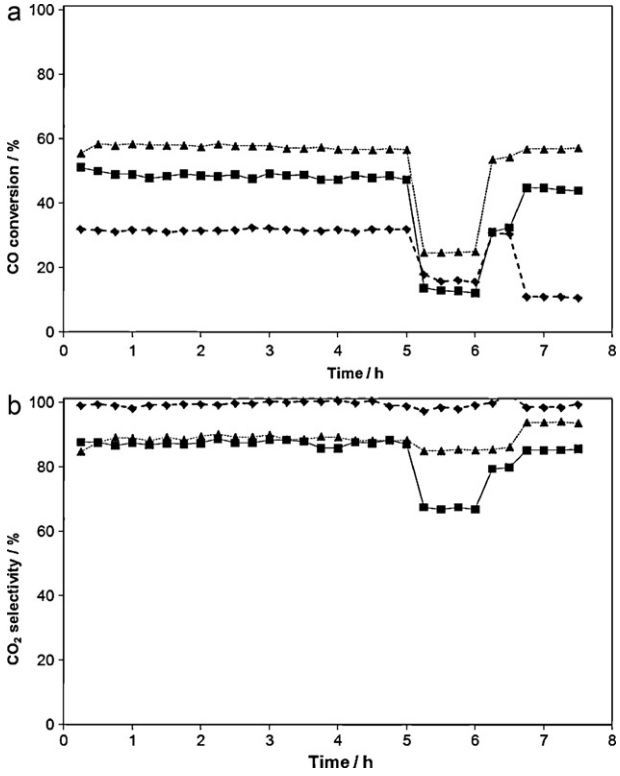

Fig. 4. Evolution of CO conversion (a) and selectivity in CO_2 (b) versus time obtained during the CO-PROX over Au/CeO_2 (10 mg) (■), Cu/CeO_2 (20 mg) (♦) and $Au\text{-}Cu/CeO_2$ (10 mg) (▲). Standard experimental conditions: 2% CO, 2% O_2, 70% H_2, 26% He, T = 100 °C, total gas inlet: 100 mL min^{-1}.

When H_2O is added, the behavior depends strongly on the catalyst. On CuO_x/CeO_2, the presence of H_2O decreases the CO conversion similarly to what is observed with CO_2, as it was demonstrated by Ratnasamy et al. [44]. On Au/CeO_2, the initial CO conversion is nearly reached, which can be explained by a cleaning of the surface and by transformation of carbonates into less stable bicarbonate species [34]. On $Au\text{-}Cux/CeO_2$ the addition of water has no significant effect.

The selectivity in CO_2 observed with the Au/CeO_2 catalyst follows the same trend as the one of CO conversion, with a decrease in selectivity when CO_2 is added in the gas feed and a recovery of the initial selectivity in presence of water. Then it can be inferred that on this catalyst, the addition of CO_2 affects only the CO conversion. For the two other catalysts, $Au\text{-}CuO_x/CeO_2$ and CuO_x/CeO_2, the addition of CO_2 or H_2O does not modify significantly the selectivity. This result is surprising, especially for the CuO_x/CeO_2 catalyst for which the CO conversion is decreased in both cases. This result could be explained by a decrease of both CO and H_2 conversion in the same extent.

4. Discussion

4.1. CO conversion at low (T < 120 °C) and high temperatures (T > 120 °C)

The kinetic results presented in Fig. 3 show that two domains of reaction should be considered: the low temperature domain (below 120 °C) and the high temperature domain (above 120 °C). Below 120 °C, the behavior of the catalyst depends essentially on their intrinsic activity in CO oxidation and the ability of CO to block H_2 oxidation. Gold–ceria is very active in both CO and H_2 oxidation and the presence of CO cannot prevent H_2 oxidation. As a consequence, a very sharp light-off of CO can be observed with a poor CO_2 selectivity (close to 50%) even when CO is not fully converted. The selectivity of gold can be improved if the reaction is carried out at very low residence time (ten times less catalyst, see Fig. 4): this means that CO oxidation occurs mainly in the first part of the catalyst bed. CuO_x/CeO_2 is less active in CO oxidation and virtually not in H_2 oxidation (100% selectivity). This excellent selectivity is very probably due to the fact that CuO_x is not reduced in Cu^0 in the reaction conditions. An intermediary behavior between pure gold and pure copper is observed for the Au-CuO_x-ceria. At 60 °C, the CO conversion is: Au/CeO_2, 88% > Au-CuO_x/CeO_2, 57% > CuO_x/CeO_2, 11% while the selectivity to CO_2 is: CuO_x/CeO_2, 100% > Au-CuO_x/CeO_2, 84% > Au/CeO_2, 47%. On this basis, the apparent rate of CO oxidation at 60 °C (mmol CO h^{-1} g^{-1}) is: Au/CeO_2, 44 > Au-CuO_x/CeO_2 28 > CuO_x/CeO_2, 5 while the apparent rate of H_2 oxidation (mmol H_2 h^{-1} g^{-1}) is: Au/CeO_2, 49 > Au-CuO_x/CeO_2 11 > CuO_x/CeO_2, 0.

In the high temperature of conversion (>120 °C), a gradual decrease of the conversion of CO can be observed on the three catalysts but this phenomenon is more marked on Au than on Cu and Au-CuO_x catalysts. Two hypotheses can be put forward to explain this behavior: (i) an increase of the ratio between the rate of H_2 oxidation and the rate of CO oxidation, (ii) the reformation of CO by the reverse water gas shift reaction (Eq. (3)). Hypothesis 1 can be discarded because the decrease of CO conversion should be linked to an inhibition of the CO oxidation reaction increasing with temperature. Such an inhibition by H_2 itself is quite unlikely and the respective effects of CO_2 and H_2O on the CO conversion over Au/CeO_2, CuO_x/CeO_2 and Au-CuO_x/CeO_2 cannot explain a strong inhibition over the Au catalyst. The second hypothesis has been evaluated by calculating the change with temperature of the equilibrium conversion of CO by the RWGS reaction. Above 120 °C for Au/CeO_2 and Au-CuO_x/CeO_2, and above 160 °C for CuO_x/CeO_2 (see Fig. 3), the gas composition following CO and H_2 oxidation is close to 2%CO_2, 2%H_2O and 68%H_2. If one let the gas reach the RWGS equilibrium, the apparent CO conversion can be calculated with temperature. The experimental results (taken from Fig. 3) and the equilibrium conversion between 120 and 300 °C are shown in Fig. 5. The actual change of the CO conversion over the Au catalyst is very close to the equilibrium conversion by RWGS. Those obtained on the copper catalysts (CuO_x and Au-CuO_x) are significantly higher than the equilibrium values. This means that the Au/CeO_2 catalyst is very active in RWGS while CuO_x/CeO_2 and Au-CuO_x/CeO_2 have not a sufficient activity to reach the RGWS equilibrium, except at the highest temperatures. The activity of Au/CeO_2 in the RWGS reaction has been demonstrated by Fourier Transformed Infra-Red spectroscopy [63].

4.2. Effect of CO_2 and H_2O

The three catalysts are inhibited by CO_2, gold being comparatively more sensitive than copper oxide. By contrast, gold-containing catalysts are relatively less sensitive than copper oxide to inhibition by steam. Gold and copper show a cooperative effect in the Au-CuO_x/CeO_2 system: though this catalyst is inhibited by CO_2, the deactivation is totally reversible; moreover, it is virtually insensitive to the presence of steam. The role of surface carbonates has been suspected in the inhibition by CO_2 while the formation of surface copper hydroxides could explain the inhibition by steam. FTIR studies are in progress to evaluate the strength of the surface carbonate species on each catalyst.

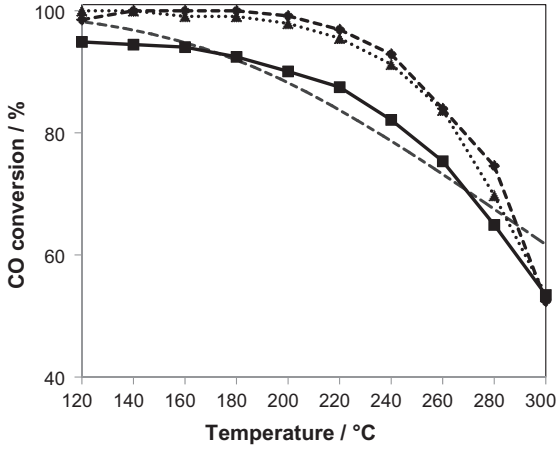

Fig. 5. Evolution of CO conversion from 120 to 300 °C in the CO-PROX reaction over Au/CeO_2 (■), CuO_x/CeO_2 (♦) and Au-CuO_x/CeO_2 (▲). The dashed line represents the equilibrium conversion by reverse water-gas shift reaction.

5. Conclusions

Gold is essentially reduced in the PROX reaction conditions while CuO_x remains in the oxidized form. In the low temperature domain (T < 120 °C) gold appears as more active than copper but much less selective. The Au-CuO_x bimetallic system has an intermediary behavior but interestingly, it has a good activity (close to that of pure gold) and a good selectivity (close to that of pure copper). All the catalysts present a maximal activity and a gradual decrease of conversion above 120 °C. This phenomenon affects more gold than copper and gold–copper catalysts. It is due to the reverse water gas shift reaction which tends to reform CO from hydrogen and CO_2. Gold is more active for this reaction, which explains the more pronounced decrease in CO conversion on this catalyst. Copper and gold–copper remains more active in this domain of temperature. An interesting cooperative effect between gold and copper is observed when CO_2 and H_2O are added to the reactants. The deactivation by CO_2 is reversible on Au-CuO_x/CeO_2 while this catalyst is virtually insensitive to the presence steam.

Acknowledgments

The authors thank the CAPES/COFECUB (project Ph603/08) for the financial support.

References

[1] J.A. Turner, Science 305 (2004) 972–974.
[2] L. Salemme, L. Menna, M. Simeone, G. Volpicelli, Int. J. Hydrogen Energy 35 (2010) 3712–3720.
[3] Y.H. Kim, E.D. Park, Appl. Catal. B: Environ. 96 (2010) 41–50.
[4] S. Monyanon, A. Luengnaruemitchai, S. Pongstabodee, Int. J. Hydrogen Energy 35 (2010) 3234–3242.
[5] P. Bera, A. Hornés, A.L. Cámara, A. Martínez-Arias, Catal. Today 155 (2010) 184–191.
[6] E.-Y. Ko, E.D. Park, K.W. Seo, H.C. Lee, D. Lee, S. Kim, Catal. Today 116 (2006) 377–383.
[7] N. Bion, F. Epron, M. Moreno, F. Mariño, D. Duprez, Top Catal. 51 (2008) 76–88.
[8] J.L. Ayastuy, A. Gurbani, M.P. González-Marcos, M.A. Gutierrez-Ortiz, Int. J. Hydrogen Energy 35 (2010) 1232–1244.

[9] S. Srinivas, E. Gulari, Catal. Commun. 7 (2006) 819–826.
[10] S. Royer, D. Duprez, Chem. Cat. Chem. 3 (2011) 24–65.
[11] S. Scire, P.M. Riccobene, C. Crisafulli, Appl. Catal. B: Environ. 101 (2010) 109–117.
[12] R.M. Heck, R.J. Farrauto, Catalytic Air Pollution Control, 2nd ed., Wiley, 2002 (Chapter 6), pp. 69–129.
[13] J.T. Kummer, Advances in Chemistry Series, vol. 143, The American Chemical Society, Washington DC, 1975, pp. 178–192.
[14] M. Kang, M.W. Song, C.H. Lee, Appl. Catal. A: Gen. 251 (2003) 143–156.
[15] J.A. Farmer, C.T. Campbell, Science 329 (2010) 933–936.
[16] S.A.C. Carabineiro, A.M.T. Silva, G. Dražić, P.B. Tavares, J.L. Figueiredo, Catal. Today 154 (2010) 21–30.
[17] D. Martin, D. Duprez, J. Phys. Chem. 100 (1996) 9429–9438.
[18] J.E. Benson, M. Boudart, J. Catal. 4 (1965) 704–710.
[19] J.E. Benson, H.S. Hwang, M. Boudart, J. Catal. 30 (1973) 146–153.
[20] F.V. Hanson, M. Boudart, J. Catal. 53 (1978) 56–67.
[21] D. Duprez, J. Chim. Phys. 80 (1983) 487–505.
[22] G.C. Bond, C. Louis, D.T. Thompson, Catalysis by Gold Catalytic Science Series, vol. 6, Imperial College Press, 2006.
[23] J.T. Miller, A.J. Kropf, Y. Zha, J.R. Regalbuto, L. Delannoy, C. Louis, E. Bus, J.A. van Bokhoven, J. Catal. 240 (2006) 222–234.
[24] T. Bligaard, J.K. Nørskov, S. Dahl, J. Matthiesen, C.H. Christensen, J. Sehested, J. Catal. 224 (2004) 206–217.
[25] D.C. Ford, A.U. Nilekar, Y. Xu, M. Mavrikakis, Surf. Sci. 604 (2010) 1565–1575.
[26] J.K. Edwards, N.E. Ntainjua, A.F. Carley, A.A. Herzing, C.J. Kiely, G.J. Hutchings, Angew. Chem. Int. Ed. 48 (2009) 8512–8515.
[27] D.I. Potemkin, P.V. Snytnikov, V.P. Pakharukova, G.L. Semin, E.M. Moroz, V.A. Sobyanin, Kinet. Katal. 51 (2010) 119–125.
[28] F. Mariño, C. Descorme, D. Duprez, Appl. Catal. B: Environ. 54 (2004) 59–66.
[29] C. Kwak, T.-J. Park, D.J. Suh, Appl. Catal. A: Gen. 278 (2005) 181–186.
[30] S.H. Oh, M.R. Sinkevitch, J. Catal. 142 (1993) 254–262.
[31] M. Schubert, M.J. Kahlich, H. Gasteiger, J. Behm, J. Power Sources 84 (1999) 175–182.
[32] T. Caputo, L. Lisi, R. Pirone, G. Russo, Appl. Catal. A: Gen. 348 (2008) 42–53.
[33] F. Arena, P. Famulari, N. Interdonato, G. Bonura, F. Frusteri, L. Spadaro, Catal. Today 116 (2006) 384–390.
[34] M. Schubert, A. Venugopal, M. Kahlich, V. Plzak, R. Behm, J. Catal. 222 (2004) 32–40.
[35] C. Galletti, S. Fiorot, S. Specchia, G. Saracco, V. Specchia, Chem. Eng. J. 134 (2007) 45–50.
[36] M. Haruta, Catal. Today 36 (1997) 153–166.
[37] W. Liu, M. Flytzani-Stephanopoulos, J. Catal. 153 (1995) 304–316.
[38] G. Avgouropoulos, T. Ioannides, Appl. Catal. A: Gen. 244 (2003) 155–167.
[39] F. Mariño, G. Baronetti, M. Laborde, N. Bion, A. Le Valant, F. Epron, D. Duprez, Int. J. Hydrogen Energy 33 (2008) 1345–1353.
[40] Y.H. Kim, E.D. Park, H.C. Lee, D. Lee, Appl. Catal. A: Gen. 366 (2009) 363–369.
[41] A. Martínez-Arias, M. Fernandez-García, J. Soria, J. Conesa, J. Catal. 182 (1999) 367–377.
[42] A. Martínez-Arias, M. Fernandez-Garcia, A.B. Hungria, A. Iglesias-Juez, O. Gálvez, J.A. Anderson, J. Catal. 214 (2003) 261–272.
[43] Y. Liu, Q. Fu, M. Flytzani-Stephanopoulos, Catal. Today 93–95 (2004) 241–246.
[44] P. Ratnasamy, D. Srinivas, C. Satyanarayana, P. Manikandan, R. Senthil Kumaran, M. Sachin, V.N. Shetti, J. Catal. 221 (2004) 455–465.
[45] S. Kacimi, J. Barbier Jr., R. Taha, D. Duprez, Catal. Lett. 22 (1993) 343–350.
[46] Y. Tanaka, T. Utaka, R. Kikuchi, K. Sasaki, K. Eguchi, Appl. Catal. A: Gen. 238 (2003) 11–18.
[47] G. Avgouropoulos, T. Ioannides, Appl. Catal. B: Environ. 67 (2006) 1–11.
[48] G. Marbán, I. López, T. Valdés-Solís, Appl. Catal. A: Gen. 361 (2009) 160–169.
[49] A. Martínez-Arias, A.B. Hungrí, G. Munuera, D. Gamarra, Appl. Catal. B: Environ. 65 (2006) 207–217.
[50] H.C. Yao, Y.F. Yu Yao, J. Catal. 86 (1984) 254–256.
[51] P. Fornasiero, J. Kašpar, V. Sergo, M. Graziani, J. Catal. 182 (1999) 56–69.
[52] E. Rocchini, M. Vicario, J. Llorca, C. de Leitenburg, G. Dolcetti, A. Trovarelli, J. Catal. 211 (2002) 407–421.
[53] S. Bedrane, C. Descorme, D. Duprez, Catal. Today 75 (2002) 401–405.
[54] F. Dong, A. Suda, T. Tanabe, Y. Nagai, H. Sobukawa, H. Shinjoh, M. Sugiura, C. Descorme, D. Duprez, Catal. Today 93–95 (2004) 827–832.
[55] T. Tabakova, F. Boccuzzi, M. Manzoli, J.W. Sobczak, V. Idakiev, D. Andreeva, Appl. Catal. A: Gen. 298 (2006) 127–143.
[56] L. Ilieva, G. Pantaleo, I. Ivanov, A. Maximova, R. Zanella, Z. Kaszkur, A.M. Venezia, D. Andreeva, Catal. Today 158 (2010) 44–55.
[57] O.H. Laguna, F. Romero Sarria, M.A. Centeno, J.A. Odriozola, J. Catal. 276 (2010) 360–370.
[58] Y. Liu, Q. Fu, M. Flytzani-Stephanopoulos, Appl. Catal. B: Environ. 27 (2000) 179–191.
[59] Y. Madier, C. Descorme, A.M. Le Govic, D. Duprez, J. Phys. Chem. B 103 (1999) 10999–11006.
[60] D. Andreeva, V. Idakiev, T. Tabakova, L. Ilieva, P. Falaras, A. Bourlinos, A. Travlos, Catal. Today 72 (2002) 51–57.
[61] G. Avgouropoulos, J. Papavasiliou, T. Tabakova, V. Idakiev, T. Ioannides, Chem. Eng. J. 124 (2006) 41–45.
[62] S. Kandoi, A.A. Gokhale, L.C. Grabow, J.A. Dumesic, M. Mavrikakis, Catal. Lett. 93 (2004) 93–100.
[63] T. Tabakova, F. Boccuzzi, M. Manzoli, D. Andreava, Appl. Catal. A 252 (2003) 385–397.